# Reaction Path of $Cu_2ZnSnS_4$ Nanoparticles by a Solvothermal Method Using Copper Acetate, Zinc Acetate, Tin Chloride and Sulfur in Diethylenetriamine Solvent

**R.B.V. Chalapathy · Gwang Sun Jung · Young Min Ko · Byung Tae Ahn* · HyukSang Kown***

Department of Materials Science and Engineering, Korea Advanced Institute of Science and Technology, 291 Daehak-ro, Yuseong-gu, Daejeon 305-701, South Korea

**ABSTRACT:** $Cu_2ZnSnS_4$ (CZTS) nanoparticles were synthesized by a solvothermal method using copper (II) acetate, zinc acetate, tin chloride, and sulfur in diethylenetriamine solvent. Binary sulfide particles such as CuS, ZnS, SnS, and $SnS_2$ were obtained at 180°C; single-phase CZTS nanoparticles were obtained at 280°C. CZTS nanoparticles with spherical shape and grain size of 40 to 60 nm were obtained at 280°C. In the middle of 180 and 280℃, CZTS and ZnS phases were found. The time variation of reaction at 280°C revealed that an amorphous state formed first instead of binary phases and then the amorphous phase was converted to crystalline CZTS state; it is different reaction path way from conventional solid-state reaction path of which binary phases react to form CZTS. CZTS films deposited and annealed from single-phase nanoparticles showed porous microstructure and poor adhesion. This indicates that a combination of CZTS and other flux phase is necessary to have a dense film for device fabrication.

**Key words:** Solvothermal, $Cu_2ZnSnS_4$,CZTS, Kesterite, Nanoparticles, Solar Cells.

## 1. Introduction

$Cu(In,Ga)Se_2$ (CIGS) solar cells show high efficiency[1]. However, due to rareness of indium and gallium on earth and their high material cost, the mass production of CIGS solar cell could be limited. Recently, $Cu_2ZnSnS_4$ (CZTS) is considered as potential alternative absorber for thin film solar cells owing to abundance of Zn and Sn and their low material cost. The CZTS shows high absorption coefficient $>10^4$/cm and p-type conductivity with direct band gap of 1.4~1.5 eV[2]. The band gap can be further controlled by adding Se in CZTS.

Various methods were used to grow CZTS films such as co-evaporation[3,4]. vapor phase sulfurization[5], electro plating/ sulfurization[6,7], spray pyrolysis[8] and soft chemistry[9,10]. So far, CZTS solar cells fabricated with vapor phase sulfurization has shown conversion efficiency 6.67%[11]. Most these processes use high vacuum systems where fabrication cost is considered as expensive. Non-vacuum process employing printing of nanoparticle-based ink has attracted much attention due to low cost and higher throughput[12]. Solar cell with efficiencies ~ 1% have been reported from CZTSSe absorbers grown with CZTS nanoparticles synthesized by hot injection and precipitation methods[13,14]. Recently, Todorov *et al.* has reported 9.96% $Cu_2ZnSn(S,Se)_4$ solar cell, prepared from a hybrid solution using hydrazine as solvent[15]. However, hydrazine is highly toxic and requires elaborate arrangements to handle it. An alternative approach to prepare nanoparticles without using toxic chemicals is solvothemal method. Solvothermal method is widely used to grow various nanostructures of $Cu(In,Ga)Se_2$[16].

By varying solvothermal conditions such as temperature, time, and types of solvent, one can modify the particle sizes and composition of the particles, which can be applied as precursor ink to grow CZTS films by low cost non-vacuum methods such as drop casting, spray coating, spin coating, and printing.

In the present work, CZTS particles were synthesized by a solvothermal method. The influence reaction temperature and reaction time on the formation and reaction path of CZTS particles and their suitability as precursors for growing CZTS absorbers were evaluated.

*Corresponding author: btahn@kaist.ac.kr, hskwon@kaist.ac.kr
Received November 29, 2013; Revised December 3, 2013; Accepted December 9, 2013

ⓒ 2013 by Korea Photovoltaic Society
This is an Open Access article distributed under the terms of the Creative Commons Attribution Non-Commercial License (http://creativecommons.org/licenses/by-nc/3.0) which permits unrestricted non-commercial use, distribution, and reproduction in any medium, provided the original work is properly cited.

## 2. Experimental

CZTS nanoparticles were grown by a solvothermal method. For the synthesis, copper (II) acetate mono hydrate, zinc acetate dihydrate, tin chloride dihydrate ($SnCl_2.2H_2O$), and sulfur powders were used. 2 mmol of Cu, 1.2 mmol of Zn, 0.8 mmol of Sn, and 4 mmol of S were mixed in a flask and they were dissolved in a 60 ml diethylenetriamine (DETA) solvent under sonication for 60 min. The solution turned from green to brownish solution indicating that metal complexes were formed and sulfur was completely dissolved. After sonication the resultant brown slurry was transferred to a teflon-lined autoclave, filled up to 70% of the volume, and kept at various temperatures and times for chemical reaction. After the reaction the autoclave was cooled to room temperature naturally and the nanoparticles in the autoclave were collected by adding ethanol followed by 5 min of centrifuge at 4,000 rpm. After centrifuge, the supernatant is decanted and the precipitate was again dispersed in 30 ml ethanol. This process was repeated for three times to remove un-reacted compounds and to disperse precipitates in ethanol.

Phases and structure of the as grown particles were determined from x-ray diffraction pattern (XRD) with Rigaku thin-film x-ray diffractometer with Cu Kα radiation (λ=1.54 Å). Morphology of the particles and composition analysis were performed with FEI NOVA 230 field-emission scanning electron microscope (FESEM) and energy dispersive spectroscopy (EDS), EDAX Genesis apex, acceleration voltage: 10 kV; collection time 100s. TEM measurement was carried out using Tecnai 300 KV High resolution transmission electron microscope (HTEM). XPS measurement was measured using a Sigma probe Thermo Scientific spectrometer.

## 3. Results and Discussions

### 3.1. CZTS particle preparation

Fig. 1 shows the XRD patterns of particles grown at various temperatures for 3 h. The XRD pattern of the particles grown at 180°C has peaks corresponding to binary sulfides including CuS, SnS, $SnS_2$, and ZnS phases. All the binary phases except ZnS phase disappear at 230 and 250°C. Figs. 1(b) and 1(c) clearly shows a peak at 28.5° that corresponds to CZTS and two peaks positioned at 26.92° and 30.52° that correspond to wurtzite ZnS. Fig. 1(d) shows CZTS peaks which correspond to Kesterite structure (JCPDS 26-0575). Note that ZnS peak disappeared at 280°C. The nanoparticles are single phase CZTS without any binary phases.

The reaction path, from Fig. 1, can be inferred as follows. First, binary phases including CuS, $SnS_2$, SnS, and ZnS formed from the solution. Second, And the CZTS phase formed from the binary phases and some ZnS phase is un-reacted. Finally, the reaction was completed with more Zn content in CZTS by absorbing un-reacted ZnS.

The composition of the CZTS particles obtained at various temperatures and times were shown in the Table 1. The particle composition indicates that the particles were Sn rich at low temperatures and the Zn content increases with increase in temperature. The reaction temperature and time are key parameters to tune the composition of nanoparticles. So far, CZTS solar cell fabricated with Cu-rich and Zn-rich absorbers have shown high conversion efficiencies[11]. The compositions of particles in Table

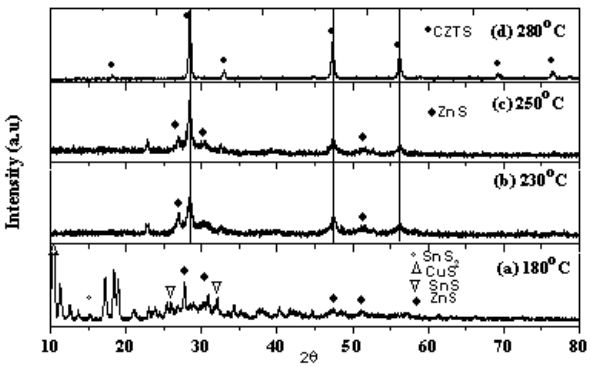


**Fig. 1.** XRD patterns of CZTS nanoparticles grown at various temperatures for 3 h

**Table 1.** Composition of CZTS particles obtained at various temperature and times

| Sample | T ℃ | t, hr | Cu (at%) | Zn (at%) | Sn (at%) | S (at%) | Cu/(Zn+Sn) | Zn/Sn | S/M |
|---|---|---|---|---|---|---|---|---|---|
| 1 | 230 | 3 | 23.2 | 9.59 | 16.48 | 50.72 | 0.89 | 0.58 | 1.03 |
| 2 | 250 | 3 | 23.56 | 12.37 | 12.64 | 51.42 | 0.94 | 0.98 | 1.06 |
| 3 | 280 | 3 | 26.32 | 14.06 | 12.54 | 47.08 | 0.99 | 1.12 | 0.89 |
| 4 | 280 | 2 | 23.74 | 12.27 | 13.3 | 50.7 | 0.93 | 0.92 | 1.03 |
| 5 | 280 | 1 | 19.72 | 14.05 | 12.84 | 53.39 | 0.73 | 1.09 | 1.05 |

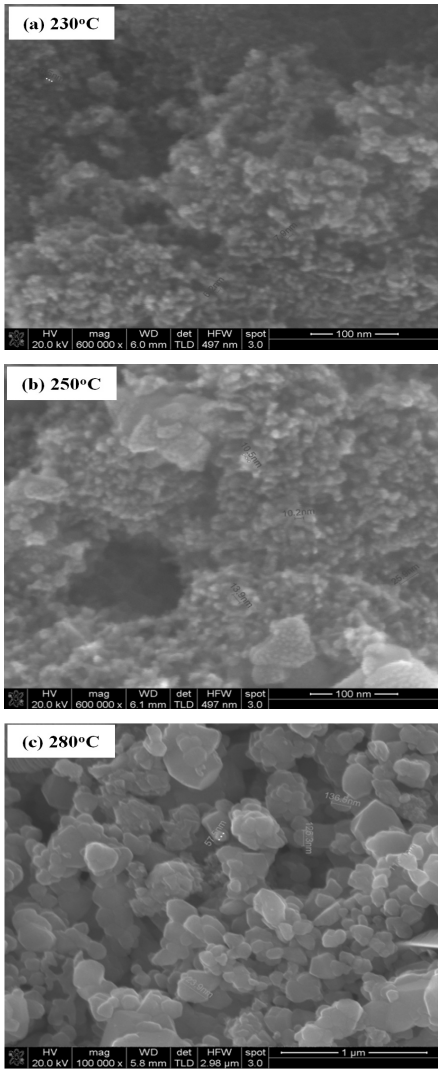


**Fig. 2.** SEM images of CZTS nanoparticles grown at 230, 250, and 280°C for 3 h

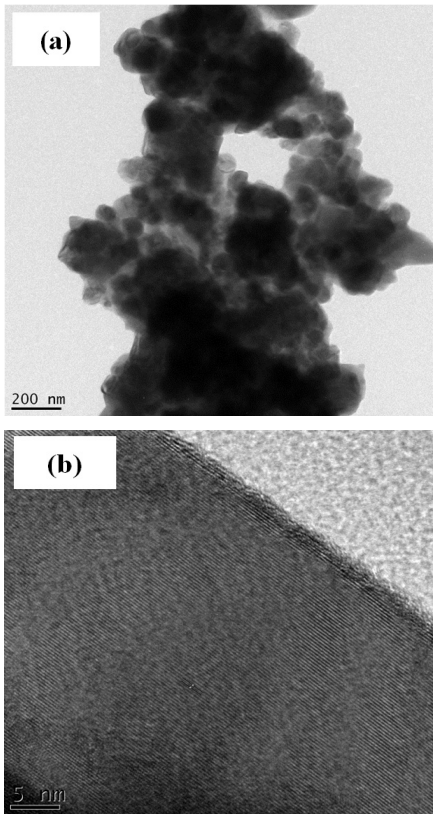


**Fig. 3.** TEM and HRTEM images of CZTS nanoparticles grown at 280°C for 3 h

1 are good agreement with CZTS particles achieved with other methods such as hot injection and precipitation methods[12, 13].

Fig. 2 shows the surface morphologies of the CZTS particles obtained at 230°C, 250°C and 280°C for 3 h. The particle size varies in the range from 10 to 20 nm for particles grown at 230 and 250°C. The particles are agglomerated at 280°C and the size of agglomerates ranged from 50 to 250 nm as seen in Fig. 2(c).

Fig. 3(a) shows TEM image of CZTS paticles synthesized at 280°C for 3 h. The size of CZTS particles is in the range 40 to 60 nm. The HTEM image in the Fig. 3(b) shows well crystallized kesterite structure. The interpalnar distance is 3.2 Å which is in agreement with the standard value of 3.13 Å for (112) plane of kesterite stucture.

However, the sizes obatined in our method is larger compared to particles obtained by other methods since the growth mechanism strongly depend on the types of solvents used in the growth of nano particles. When oleyamine was used as slovent spherical-shaped particles with sizes about 5-25 nm were obtained[12,13]. However, when DETA is used as solvent nanoparticles with spherical shape as well as rod-like shape form due different solvent-template mechnism[16].

In order to identify the chemical state of the elements in the particles, XPS measurement was performed on the CZTS particles grown at 280°C for 3 h. The survey spectrum of the sample indicated that CZTS particles consist of carbon and oxygen as impurities.

Fig. 4 shows the XPS spectra of the CZTS particles grown at 280°C for 3 h. The C1s peak appeared at 286.2 eV due to shift from the original position 284.5 eV. All the peaks positions were measured with respect to C 1s. Cu peaks appeared at binding energies 932.24 and 952.04 eV for Cu $2p_{3/2}$ and $2p_{1/2}$ respectively. The difference in the peak splitting is 19.8 eV suggesting that Cu is in Cu(I) state. Peaks corresponding to Zn $2p_{3/2}$ and Zn $2p_{1/2}$ are positioned at 1022.21 and 1045.31 eV, respectively. The separation between these peaks is 23.1 eV, which is in agreement with the standard separating of 23 eV indicating Zn is in Zn(II) state.

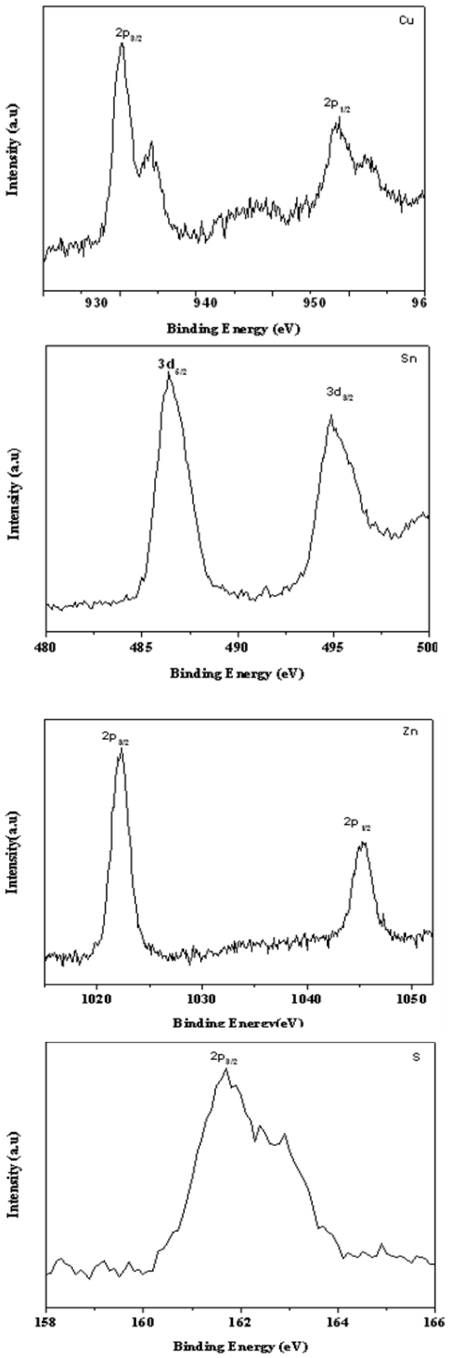


**Fig. 4.** XPS spectra of CZTS nanoparticles grown at 280°C for 3 h

Sn peaks corresponding to $Sn3d_{3/2}$ and $Sn3d_{5/2}$ are positioned at 486.44 and 494.89 eV, respectively. The difference in the peak splitting is 8.45 eV, which agrees well with standard splitting of 8.4 eV, indicates that Sn is in Sn(IV) state. S 2p peaks at 161.69 and 162.91 eV agree well with the standard binding energy values of 160-163 eV, suggesting that sulfur is in the form of sulfide in the particles.

Fig. 5 shows XRD patterns of the nanoparticles obtained at 280°C with various reaction times. After 1-h reaction, nanoparticles

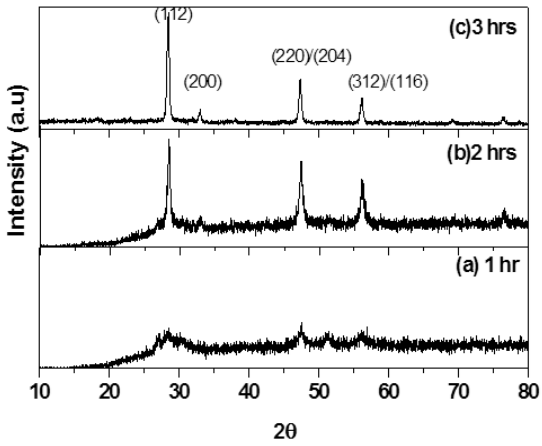


**Fig. 5.** XRD patterns of CZTS nanoparticles grown at 280°C for 1, 2, and 3 h. Note amorphous phase was formed in early stage and no binary or ternary phase was detected

taken from sample showed a broad pattern with much noise; this indicates that the structure of nanoparticles is in an amorphous state. It seems that the amorphous state at 280°C is an indication of early form of CZTS reaction with CZTS major peaks. No binary phases such as CuS, SnS, $SnS_2$, and ZnS were detected at this temperature even though the reaction was not completed; it suggests that an amorphous CZTS phase was immediately formed instead of forming binary or ternary phase at early stage of reaction at 280°C. After 2-h reaction, CZTS phase clearly appears; but amorphous phase also exists. After 3-h reaction, the base-line noise intensity is very small, indicating that the reaction is completed and single-phase CZTS is formed. The result indicates that the reaction path is different from the solid-state sintering process where $Cu_2SnS_3$ phase forms first.

DETA solvent used in our experiment acts as strong reducing agent. The complexing agent forms amine complexes with metal cations. At low temperature reaction, $S^{2-}$ anions react with cations released from the amine metal complexes to form binary sulfides such as CuS and $SnS_2$ and ZnS, shown in Fig. 1. As the reaction temperature increased these binaries react to form CZTS particles in an amorphous state first and then converted to crystalline state. At 250°C, the reaction mechanism could follow the reaction path of solid-state reaction between $Cu_2SnS_3$ and ZnS[17].

However, in direct reaction at 280°C, the reaction path seemed different. In the early stage at 280°C, no $Cu_2SnS_3$ or ZnS was found. Also no CZTS phase was found. Instead, an amorphous CZTS was formed and slowly converted into crystalline CZTS. So the reaction path at 280°C is different from solid-state

reaction. It is assumed that amine metal complex react with $S^{2-}$ ions but the reaction is fast enough so that amine complex is incorporated into nanoparticles. As a result, nanoparticles are in amorphous state and the composition is similar to bulk solution content. It takes 2 h for complete transformation from amorphous state into CZTS.

### 3.2. CZTS film deposition

To deposit CZTS films, an ink was prepared by adding 3 ml terpinol organic binder to 250 mg CZTS nanoparticles, obtained at 280°C and sonicated for 1 h. The prepared ink was coated onto Mo-coated glass substrates by drop casting and was dried at 150°C for 10 min on the hot plate. Then, the film was annealed at 350°C in Ar. The cross section of the CZTS film deposited is shown in Fig. 6. The thickness of the film was about 32 μm. The film shows very small CZTS grains with many voids, suggesting that sintering temperature was not high enough. The contents of Cu, Zn, Sn, and S are 27.7, 11.8, 13.3, and 48.2% respectively; it is slightly Cu and Sn rich.

The film contains carbon, which results from incomplete volatilization of the binder. The films showed very poor adhesion, probably due to no interface reaction between CZTS and Mo at such low temperature. CZTS films prepared by annealing at 530°C for 30 min in sulfur atmosphere in a graphite box also showed poor adhesion.

In order to obtain a dense CZTS film with large grains, a flux (or second phase) that can melt at sintering temperature should be added in the ink. Flux material can be added during CZTS film preparation or during film fabrication. Further optimization of ink by adding appropriate flux is the next approach and is beyond the scope of this paper.

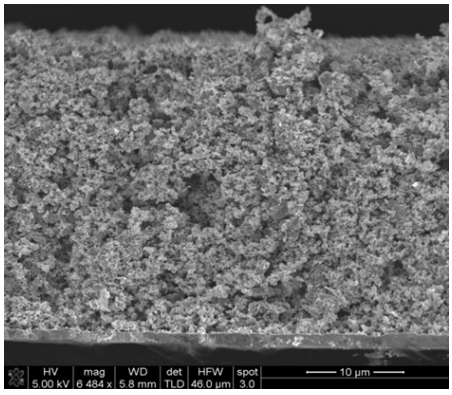


**Fig. 6.** Cross-sectional SEM image of CZTS film after annealing in Ar at 350°C for 30 min

## 4. Conclusions

CZTS nanoparticles were synthesized by a solvothermal method using copper acetate, zinc acetate, tin chloride, and S in DTEA solvent. At 180°C reaction, binary sulfide phases such as CuS, SnS, $SnS_2$, and ZnS were formed and no CZTS was detected. At 280°C, CZTS particles with no other phase were grown and the particle size was in the range of 40 to 60 nm. From temperature dependence of CZTS formation, the reaction path was consistent with solid-state sintering process where binary phases form first and reacted to CZTS phase. But 280C reaction with time variation showed that an amorphous phase was formed instead of binary phases; the amorphous phase was converted to crystalline CZTS phase. So the reaction path is different from the solid-state sintering mechanism.

CZTS films obtained by annealing at 350 and 530°C with mixture of nanoparticles and terpinol organic binder exhibited many voids and poor adhesion. It is necessary to add a flux material into paste or prepare nanoparticles with a low-temperature melting phase to obtain a dense and large-grained film for solar cell application.

## Acknowledgments

This work was supported by the center for Inorganic Photovoltaic Materials (No. 2012-0001167), the Priority Research Center Program (2011-0031407) funded by the Korean Ministry of Education, Science, and Technology, and Project KIERD22411 funded by the Korea Institute of Energy Research.

## References

1. M. A. Green, K. Emery, Y. Hishikawa, and W. Warta, "Solar cell efficiency tables (version 36)", *Prog. Photovolt: Res. Appl.* 18, 144–150 (2010).
2. K. Ito and T. Nakazawa, "Electrical and optical properties of stannite-type quaternary semiconductor thin films", *Jpn. J. Appl. Phys*, 27, 2094-2097 (1988).
3. T. M. Friedlmeier, N. Wieser, T. Walter, H. Dittrich, H. W. Schock, *Proceedings of the 14th EPVSEC*, P4B.10 (1997).
4. B. A. Schubert, B. Marsen, S. Cinque, T. Unold, R. Klenk, S. Schorr, and H. W. Schock, "$Cu_2ZnSnS_4$ thin film solar cells by fast coevaporation", *Prog. Photovolt: Res. Appl.* , 19, 93-96 (2011).
5. H. Katagiri, "$Cu_2ZnSnS_4$ thin film solar cells", *Thin Solid*

*Film*, 480, 426-432 (2005).

6. J. J. Scragg, D. M. Berg, and P. J. Dale, "A 3.2% efficient Kesterite device from electrodeposited stacked elemental layers", *J. Electroanalytical Chemistry*, 646, 52-59 (2010).
7. R. Schurr, A. Holzing, S. Jost, R. Hock, T. Voss, J. Schulze, A. Kirbs, A. Ennaoui, M. Lux-Steiner, A. Weber, I. Kotschau, H.W. Schock, "The crystallization of $Cu_2ZnSnS_4$ thin film solar cell absorbers from co-electroplated Cu-Zn-Sn precursors", *Thin Solid Films*, 517, 2465-2468 (2009).
8. N. Kamoun, H. Bouzouita, B. Rezig, "Fabrication and characterization of $Cu_2ZnSnS_4$ thin film deposited by spray pyrolysis technique", *Thin Solid Films*, 515, 5949–5952 (2007).
9. T. Todorov, M. Kita, J. Carda, P. Escribano, "$Cu_2ZnSnS_4$ films by deposited by a soft-chemistry method", *Thin Solid Films*, 517, 2541–2544 (2009).
10. K. Tanaka, N.Moritake, M. Oonuki, H.Uchiki, "Pre-annealing of precursors of $Cu_2ZnSnS_4$ thin films prepared by sol-gel sulfuring method", *Jpn. J. Appl. Phys*. 47, 598-601 (2008).
11. H. Katagiri, K. Jimbo, S. Yamada, T. Kamimura, W.S. Maw, T. Fukano, T. Ito, T. Motohiro, "Enhanced conversion efficiencies of $Cu_2ZnSnS_4$ based thin film solar cells by using preferential etching technique", *Applied Physics Express*, 1, 041201 (2008).
12. J. K. J. van Duren, C. Leidholm, A. Pudov, M.R. Robinson, Y. Rossillon, *Mat. Res. Soc. Sym. Proc*. 2007, 1012,Y05-03.
13. Q. Guo. H. W. Hillhouse, R. Agrawal, "Synthesis of $Cu_2ZnSnS_4$ nanocrystal ink and its use for solar cells", *J. Am. Chem. Soc.*, 131, 11672 (2009).
14. C. Steinhagen, M. G. Phatani, V. Akhavn, B. Goodfellow, B. Koo, B. A. Korgel, "Synthesis of $Cu_2ZnSnS_4$ nanocrystal for use in low-cost photovoltaics", *J. Am. Chem.*, Soc 131, 12554 (2009).
15. T. K. Todorov, K. B. Reuter, D. B.Mitizi, "High-efficiency solar cell with earth-abundant liquid-processed absorber", *Adv. Mater.*, 22, E156 (2010).
16. K. H. Kim, Y. G. Chun, B. O. Park, K. H. Yoon, *Materials Science Forum*, 449-452 (2004).
17. F. Hergert, R. Hock, "Predicted formation reaction for the solid-state synthesis of the semiconductor materials $Cu_2SnX_3$ and $Cu_2ZnSnX_4$ (X=S, Se) starting from binary chalcogenides", *Thin Solid Films*, 515, 5953-5956 (2007).